Strong nonlinear dynamic rupture theory of thin liquid films

Chi-Chuan Hwang, Jun-Liang Chen, and Li-Fu Shen
Department of Mechanical Engineering, Chung Yuan University, Chung-Li, Taiwan 32023, Republic of China
(Received 21 February 1996; revised manuscript received 29 April 1996)

This research studies the strong nonlinear rupture phenomena of a thin liquid film on a horizontal plane. The strong nonlinear evolution equations are obtained by the Kármán-Polhausen integral method with a specified velocity profile. These evolution equations are used to investigate the rupture process for liquid films. The numerical results show that although the inertia accelerates the rupture process explicitly, the high-order viscous dissipation reduces this acceleration. [S1063-651X(96)04709-5]

PACS number(s): 66.60.+a, 68.15.+e, 02.60.Cb, 02.70.Bf

Research of the rupture of a thin liquid film has been motivated by industrial applications in disperse and, colloid systems on the one hand, and an understanding of diverse biological implications on the other [1–3]. A liquid layer on a solid substrate may be unstable when the thickness of the layer becomes very thin (100–1000 Å). To explain the mechanism of the instability of a thin liquid film, Sheludko [4] proposed an idea of the negative disjoining pressure induced by the long-range molecular forces due to the van der Waals potential (VDWP). In the case of a thin film on a solid substrate, the critical wavelength and the linear rupture time of the thin film, which are related to the surface tension and the van der Waals potential, can be obtained by the hydrodynamic stability theory [5–7]. Williams and Davis [8], Burelbach *et al.* [9] and Hwang *et al.* [10] analyzed the long-wave nonlinear dynamic rupture of film on a plate. They found that the nonlinearity accelerates the rupture process. Furthermore, Chen and Hwang [11] indicated that the inertial effect of the longitudinal momentum equation accelerated the rupture process explicitly.

In the research mentioned above, some high-order terms in the governing equations and the boundary conditions are neglected. However, these terms are explicit during the strong nonlinear period of the rupture process [10]. In the present work, the order of magnitude of each physical effect is estimated and the reduced governing equations are obtained. Sequentially, the integral method [12,13] is used to derive a system of strong nonlinear evolution equations. Then the numerical results of the evolution equations are compared with the Williams and Davis's equations (WDE) [10] and Chen and Hwang's equations (CHE) [11].

A planar thin liquid film on a horizontal plane is shown schematically in Fig. 1. The liquid is assumed to be a Newtonian viscous fluid with kinematic viscosity ν and constant density ρ. It is also assumed that the liquid film discussed here is thin enough to neglect the gravity effect and only the effect of VDWP is considered. By scaling the coordinate by the equilibrium thickness h_0, time by h_0^2/ν, velocity by ν/h_0, and pressure by $\rho\nu^2/h_0^2$, the modified Navier-Stokes equations are given by [7]

$$u_t+uu_x+wu_z=-p_x-\phi_x+u_{xx}+u_{zz}, \tag{1}$$

$$w_t+uw_x+ww_z=-p_z-\phi_z+w_{xx}+w_{zz}, \tag{2}$$

$$u_x+w_z=0, \tag{3}$$

simultaneously with the boundary conditions:
at $z=h$,

$$(u_z+w_x)-4u_xh_x(1-h_x^2)^{-1}=0, \tag{4}$$

$$-p+2[(1-h_x^2)w_z-h_x(u_z+w_x)](1+h_x^2)^{-1} = 3Sh_{xx}(1+h_x^2)^{-3/2}; \tag{5}$$

at $z=0$,

$$u=w=0, \tag{6}$$

and also with the kinematic condition at the free surface given by

$$h_t+uh_x=w, \tag{7}$$

where u, w, and p are the dimensionless x-component velocity, the z-component velocity, and pressure, respectively, and the subscripts represent partial derivatives. The attractive van der Waals forces are obtained through the potential function ϕ, which depends on the film thickness as $\phi=Ah^{-3}$. The dimensionless parameters A and S are defined as

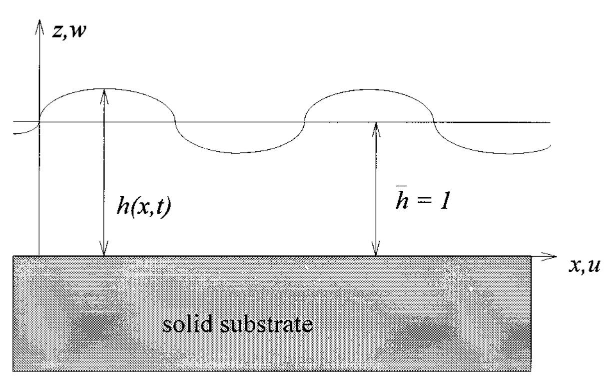

FIG. 1. The physical model of a thin liquid film.

$A = A'/(6\pi h_0 \rho \nu^2)$ and $S = h_0 \sigma/(3\rho\nu^2)$, where A' is the dimensional Hamaker constant, and σ is the dimensional surface tension.

After solving the linear stability problem of Eqs. (1)–(7) (please refer to the Appendix for details), one can find the neutral state of the system that occurs at the cutoff wave number as

$$k_c = \left(\frac{A}{S}\right)^{/12}. \tag{8}$$

It is clear that only disturbances with wave numbers below the cutoff wave number are unstable. Since the real orders of magnitude of A and S are small [8,9], some high-order terms in the governing equations and the boundary conditions must be concluded in the reduced system in which we expect to take A and S into consideration. We assume that the order of magnitude of A and S are $S = O(\epsilon)$ and $A = O(\epsilon^4)$, where ϵ is a relatively small parameter. Introducing the above two dimensionless parameters into Eq. (9), the order of unstable wave number k can be represented as

$$k = O(\epsilon^{3/2}). \tag{9}$$

The orders of other dimensionless variables are given by [8,9]

$$u = O(1), \quad w = O(k), \quad p = O(k^{-1}),$$

$$x = O(k^{-1}), \quad z = O(1), \quad t = O(k^{-1}). \tag{10}$$

Introducing Eqs. (9) and (10) into Eqs. (1)–(7) and neglecting the higher terms of order higher than $O(\epsilon^6)$, the reduced equations of motion and the pertinent boundary conditions can be derived as follows:

$$u_t + uu_x + wu_z = -p_x - \phi_x + u_{xx} + u_{zz}, \tag{11}$$

$$w_t + uw_x + ww_z = -p_z + w_{zz}, \tag{12}$$

$$u_x + w_z = 0; \tag{13}$$

at $z = h$,

$$u_z = 4u_x h_x - w_x, \tag{14}$$

$$-p - 3Sh_{xx} = 2u_x + 2u_z h_x, \tag{15}$$

$$h_t + uh_x = w; \tag{16}$$

and at $z = 0$

$$u = w = 0. \tag{17}$$

The high-order viscous dissipation terms are the normal stress in x-momentum equations, shear stress in z-momentum equations, and the interfacial shear and normal stress on the right-hand side of the dynamic boundary conditions [(14) and (15)] that are caused by a large interface deformation. The above high-order terms become important as the rupture process reaches the nonlinear stage.

One can obtain the mass balance relationship by rewriting Eq. (16) as

$$h_t + \frac{\partial}{\partial x}\int_0^h u\,dz = h_t + q_x = 0, \tag{18}$$

where q is the local flow rate. A specific profile must be imposed in the integral method. For a highly turbulent flow, a flat profile is usually assumed. However, for the flow of interest here, a parabolic profile established experimentally by Alekseenko *et al.* [12] is more appropriate. Therefore, we impose the following second-order self-similar profile of u as

$$u = \frac{3q}{h}\left[\left(\frac{z}{h}\right) - \frac{1}{2}\left(\frac{z}{h}\right)^2\right] - \frac{fh}{2}\left[\left(\frac{z}{h}\right) - \frac{3}{2}\left(\frac{z}{h}\right)^2\right], \tag{19}$$

where $f(x,t)$ is an unknown correlation function. This velocity profile satisfies the no-slip condition at the solid boundary and $u_z = f(x,t)$ at the free surface. Applying the continuity equation and Eq. (19), Eq. (14) becomes

$$f = 4G_x h h_x + 4L_x h^2 h_x + \tfrac{1}{2}G_{xx}h^2 + \tfrac{1}{3}L_{xx}h^3, \tag{20}$$

where $G = 3qh^{-2} - 0.5f$ and $L = -1.5qh^{-3} + 0.75fh^{-3}$. Equation (20) represents the nonlinear shear stress equilibrium relation at the interface and the unknown function f correlates to h and q in the rupture process. Furthermore, integrating Eq. (11) over the film and applying the other boundary conditions, one can obtain the averaged x-momentum equation as

$$\begin{aligned} q_t &+ (\tfrac{1}{3}G^2h^3 + \tfrac{1}{2}GLh^4 - \tfrac{1}{5}L^2h^5)_x \\ &= 3Shh_{xxx} + 3Ah^{-3}h_x - 3qh^{-2} + \tfrac{3}{2}f + \tfrac{1}{2}G_{xx}h^2 \\ &\quad + \tfrac{1}{3}L_{xx}h^3 + 2h(Gh)_{xx} + 2h(Lh^2)_{xx} + \{\tfrac{1}{8}G_{xt}h^4 \\ &\quad + \tfrac{1}{15}L_{xt}h^5 - \tfrac{1}{2}G_xh^2 - \tfrac{2}{3}L_xh^3 + \tfrac{1}{10}[(GG_x)_x \\ &\quad - 2G_x^2]h^5 + \tfrac{1}{36}[3(LG_x) + 2(GL_x)_x - 10G_xL_x]h^6 \\ &\quad + \tfrac{1}{21}[(LL_x)_x - 2L_x^2]h^7\}_x. \end{aligned} \tag{21}$$

Equations (18), (20), and (21) are the coupled nonlinear evolution equations about the film thickness h, local flow rate q, and the correlation function f, respectively. Here, Eqs. (18), (20), and (21) are referred to as the SNE. If one derives an evolution equation to retain the physical effects up to $O(\epsilon^6)$ by a long-wave expansion method [8], it will contain most of the high-order viscous dissipation effects included in the SNE. However, this equation will be too complicated to analyze either numerically or analytically.

The nonlinear rupture process of the system is revealed first by solving the SNE numerically. Equations are discretized by using the finite difference method. Center differences are applied in space while the Crank-Nicolson rule is used for time. The calculation domain is fixed in the interval $0 \leqslant x \leqslant 2\pi/k_m$, where k_m is the wave number on which the linear maximum growth rate is achieved. The periodic boundary conditions are considered in this problem. The initial-value conditions are

$$h(x,0) = 1 + H_0 \cos k_m x, \quad 0 \leqslant x \leqslant 2\pi/k_m, \tag{22}$$

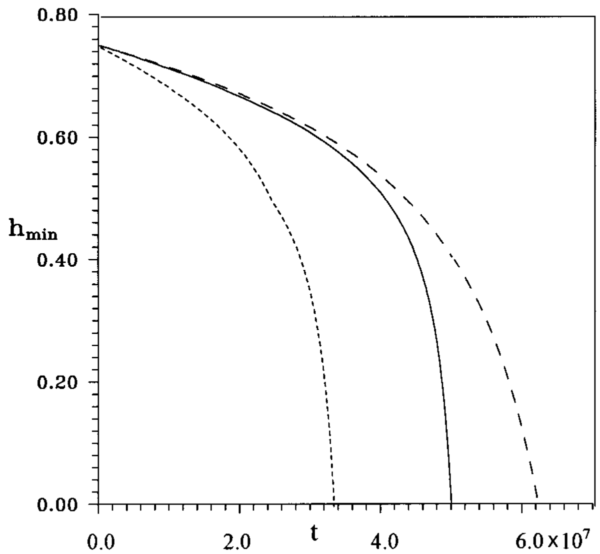

FIG. 2. The minimum film thickness, $h_{\min}$, versus time for $S=0.1$ and $A=0.000\,05$: —, SNE; – –, WDE; ---, CHE.

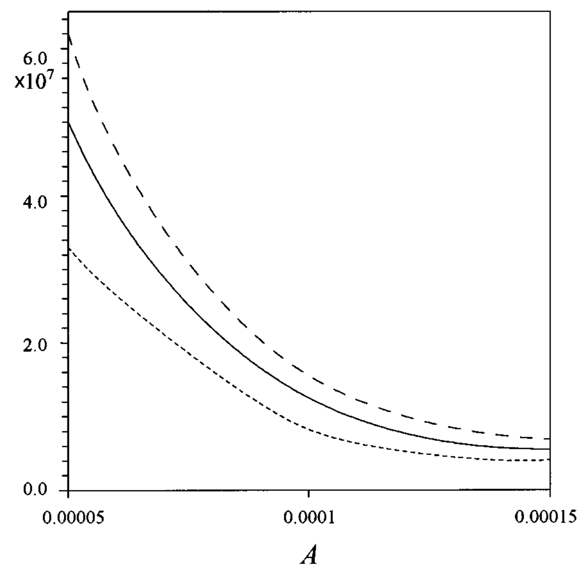

FIG. 3. Nonlinear rupture time versus A of three models for $S=0.1$: —, SNE; – –, WDE; ---, CHE.

$$q(x,0)=-\frac{\omega_m}{k_m}H_0\sin k_m x,\quad 0\leqslant x\leqslant 2\pi/k_m, \tag{23}$$

where ω_m is the linear maximum growth rate and H_0 is the initial disturbance. The initial condition for f is obtained by solving the discretized system of Eq. (23) with the initial conditions of h and q. The Newton-Raphson iteration method is introduced to calculate the difference equations and the convergent tolerance is around 10^{-5}. In the cases mentioned below, the initial disturbance H_0 is 0.25.

Figure 2 displays the nonlinear rupture processes predicted by the WDE, CHE, and SNE, respectively, with different values of A; $h_{\min}$ is the minimum film thickness during the rupture process. One can observe that the rupture process is accelerated when the $h_{\min}$ approaches the solid boundary. It is also shown that the rupture process predicted by the SNE is faster than that predicted by WDE but slower than that predicted by CHE. It is clear that the inertia of x-momentum equations will accelerate the rupture process while the high-order viscous dissipation effects will reduce this acceleration. This tendency is also shown in Fig. 3. Figure 3 shows the rupture times vs A of three models for $S=0.1$. The rupture time predicted by the WDE (CHE) is longer (shorter) than that predicted by the SNE by about 24% (26%) in the case of $S=0.1$, $A=0.000\,15$, while in the case of $S=0.1$ and $A=0.000\,05$ the difference is about 24% (36%). For the large difference in the predicted rupture times, one can say that the high-order viscous dissipation consumes some energy that is used to make the film rupture, and is not negligible in modeling the film rupture process. In the meantime, the larger the value of A, the shorter the rupture time predicted by the nonlinear analysis. That is, the film tends to be unstable as the effect of VDWP is enlarged. This phenomenon can also be shown by Eq. (8). The neutral state, or cutoff wave number k_c of the system is increased with the A value being increased. The larger the k_c value means the stronger the destability of the system. On the contrary, the k_c is decreased with the S value increasing, and the system tends to be stable.

In summary, it is concluded that VDWP and the inertia of x-momentum equations are the unstable factors, while the surface tension and high-order viscous dissipation are the stable factors for the instability of the film. They are all important in the simulation of rupture processes of thin liquid films. It is noticeable that the modified Navier-Stokes equations may not be a valid model when the film becomes exceedingly thin, in which case the film is no longer Newtonian [8].

The authors wish to acknowledge with appreciation the financial support (Grant No. NSC 82-0401-E033-020) provided by the National Science Council of the Republic of China.

APPENDIX

The base states of Eqs. (1)–(7) are

$$\overline{u}=0,\quad \overline{w}=0,\quad \overline{h}=1.$$

We assume the perturbation of the velocity vector (u',w'), the pressure p', and the height of free surface h' have the form

$$(u',w',p',h')=[\hat{u}(z),\hat{w}(z),\hat{p}(z),a]\exp(\omega t+ikx), \tag{A1}$$

where k is the wave number and ω is the complex characteristic value.

Taking Eq. (A1) into account, the linearized governing equations can be conveniently reduced to a single Orr-Sommerfeld equation for $\hat{w}(z)$:

$$[D^4-(2k^2+\omega)D^2+k^2(k^2+\omega)]\hat{w}=0, \tag{A2}$$

and the boundary conditions (4)–(7) become

$$\hat{w}=D\hat{w}=0 \quad (\text{at } z=0), \tag{A3}$$

$$\hat{w}=a\omega \quad (\text{at } z=1), \tag{A4}$$

$$(D^2+k^2)\hat{w}=0 \quad (\text{at } z=1), \tag{A5}$$

$$[D^3-(3k^2+\omega)D+3k^2\omega^{-1}(A-Sk^2)]\hat{w}=0 \quad (\text{at } z=1), \tag{A6}$$

where D denotes d/dz.

After calculating the solution of Eq. (A9) with boundary conditions (A3)–(A6), the secular determinant would lead to a relation among the parameters in the following form:

$$\begin{aligned}\mathcal{F}(\omega,k,A,S)=&2\beta_1\beta_2(4k^4+2k^2\omega)\\&+k^2(8k^4+8k^2\omega+\omega^2)\sin\beta_1\sin\beta_2\\&-3k^2\beta_2(A-Sk^2)\sin\beta_1\cos\beta_2\\&-\beta_1\beta_2(8k^4+4k^2\omega+\omega^2)\cos\beta_1\cos\beta_2\\&+3k^2\beta_1(A-Sk^2)\cos\beta_1\sin\beta_2=0,\end{aligned} \tag{A7}$$

where $\beta_1^2=-(k^2+\omega)$ and $\beta_2^2=-k^2$. The neutral state of the system implies that the real part of ω is zero, and from Eq. (A7) it is easy to find the cutoff wave number shown in Eq. (8).

[1] D. A. Edwards, H. Brenner, and D. T. Wasan, *Interfacial Transport Process and Rheology* (Butterworth-Heinemann, London, 1991).

[2] D. Myers, *Surfaces, Interfaces, and Colloids* (VCH, New York, 1991).

[3] J. T. G. Overbeek, J. Phys. Chem. **64**, 1178 (1960).

[4] A. Sheludko, Adv. Colloid Interface Sci. **1**, 391 (1967).

[5] P. G. de Gennes, Rev. Mod. Phys. **57**, 827 (1985).

[6] A. Vrij, Discuss. Faraday Soc. **42**, 23 (1966).

[7] E. Ruckenstein and R. K. Jain, J. Chem. Soc. Faraday Trans. 2 **70**, 132 (1974).

[8] M. B. Williams and S. H. Davis, J. Colloid Interface Sci. **90**, 220 (1982).

[9] J. P. Burelbach, S. G. Bankoff, and S. H. Davis, J. Fluid Mech. **195**, 463 (1988).

[10] C.-C. Hwang, S.-H. Chang, and J.-L. Chen, J. Colloid Interface Sci. **159**, 184 (1993).

[11] J.-L. Chen and C.-C. Hwang, J. Colloid Interface Sci. **167**, 214 (1994).

[12] S. V. Alekseenko, V. Ye. Narkoryakov, and B. G. Pokusaev, AIChE J. **31**, 1446 (1985).

[13] Th. Prokopiou, M. Cheng, and H.-C. Chang, J. Fluid Mech. **222**, 665 (1991).